Underwater Acoustic Sparse Aperture System Performance: Using Transmitter Channel State Information for Multipath & Interference Rejection

Andrew Puryear,* Lisa J. Burton,[†] Pierre F.J. Lermusiaux,[†] and Vincent W.S. Chan*

*Claude E. Shannon Communication and Network Group
Massachusetts Institute of Technology, Cambridge, MA 02139
[†]Multidisciplinary Simulation, Estimation, and Assimilation Systems (MSEAS)
Massachusetts Institute of Technology, Cambridge, MA 02139
Email: puryear@mit.edu

Abstract—Today's situational awareness requirements in the undersea environment present severe challenges for acoustic communication systems. Acoustic propagation through the ocean environment severely limits the capacity of existing underwater communication systems. Specifically, the presence of internal waves coupled with the ocean sound channel creates a stochastic field that introduces deep fades and significant intersymbol interference (ISI) thereby limiting reliable communication to low data rates. In this paper we present a communication architecture that optimally predistorts the acoustic wave via spatial modulation and detects the acoustic wave with optimal spatial recombination to maximize reliable information throughput. This effectively allows the system to allocate its power to the most efficient propagation modes while mitigating ISI. Channel state information is available to the transmitter through low rate feedback. New results include the asymptotic distribution of singular values for a large number of apertures. Further, we present spatial modulation at the transmitter and spatial recombination at the receiver that asymptotically minimize bit error rate (BER). We show that, in many applications, the number of apertures can be made large enough so that asymptotic results approximate finite results well. Additionally, we show that the interference noise power is reduced proportional to the inverse of the number of receive apertures. Finally, we calculate the asymptotic BER for the sparse aperture acoustic system.

I. INTRODUCTION

The ocean is a challenging environment for transmission of data, with channel reverberation in both time and frequency [1] limiting data rate. Surface waves, small scale turbulence and fluctuations of physical properties generate random signal variation that creates deep fades and limits reliable communication. Previous work [2] has established three characteristics of the underwater acoustic channel that distinguish it from other wireless channels: frequency-dependent propagation loss, multipath, and low speed of sound (1500 m/s).

Because of frequency dependent propagation loss, different communication architectures are appropriate for different transmission ranges (also called *link ranges*). Over very short link ranges (under 100m), optical wireless communication is usually appropriate, providing reliable high rate communication. Underwater optical systems are limited beyond 100m because optical energy is quickly attenuated due to absorption
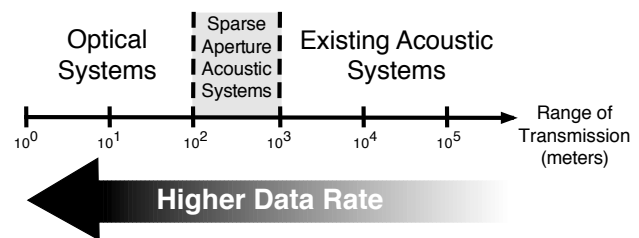

Fig. 1. Optical wireless communication systems are extremely limited in distance. Data rate is comprised for distance of transmission.

and scattering. Optical communication in the ocean is even more limited in turbid or turbulent water [3].

For link ranges beyond the limit of optical communication, high frequency acoustic systems are appropriate. These systems provide high data rate and reliable communication by transmitting in the 10-30kHz band. The usable frequency band for high frequency, short range acoustic systems is restricted primarily by channel attenuation and transducer bandwidth [2]. In practice, high frequency acoustic systems are limited beyond 1km because of significant path loss. Thus, for long link ranges low frequency acoustic systems are appropriate, providing reliable communication where optical or high frequency acoustic systems suffer from too much attenuation to be useful. The three regions (short range, intermediate range, and long range) along with the optimal architecture for each region is shown in Fig. 1. The region labeled *optical systems* corresponds to the short range region, *sparse aperture acoustic systems* corresponds to the intermediate range region (high frequency acoustics), and *existing acoustic systems* corresponds to the long range region (low frequency acoustics). This paper focuses on the intermediate range: we propose an architecture for efficient communication in this high frequency intermediate range region.

For the intermediate range, refraction and reflection can cause the transmitted signal to reach the receiver by two or more paths. This phenomenon, called multipath, causes intersymbol interference (ISI) and signal fading [4], thus pre-
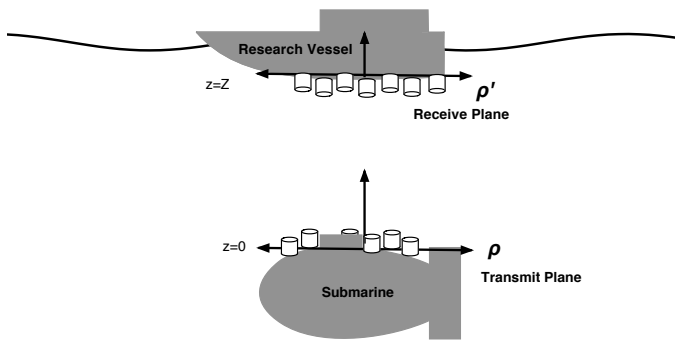
Fig. 2. One application of short range acoustic communication is data transfer between a submarine and a research vessel on the sea surface. Here, a transmit plane array of apertures on a submarine communicates to a receive plane on a research vessel.
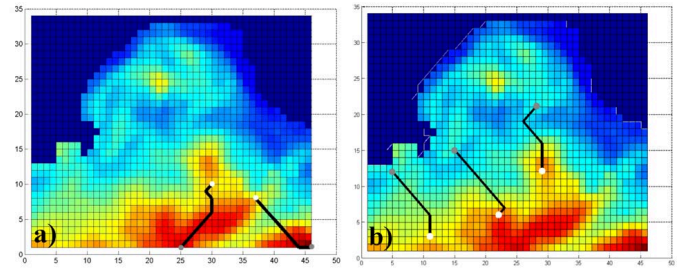

Fig. 3. Example of adaptive sampling requiring vehicles/surface-craft/shore communications. Illustrated are sampling paths generated for fixed 2-D objective fields using Mixed-Integer Programming. The background maps are proportional to error standard deviation. Grey dots are starting points for the AUVs and white dots are the computed optimal termination points. (a) Optimal path of two vehicles and (b) three vehicles [15]. The question answered is "assuming the error field remains constant for the next day, on which path do I send my AUVs?."

senting significant challenges in signal transmission. Multipath generally is strongest for horizontal channels [2]. Reflections and refraction that cause multipath are particularly problematic when the channel includes a boundary (either air-sea or sea-sea floor) or is within the "deep" sound channel created by the background sound speed profile. Current work reports the use of equalizers or vector receivers to mitigate multipath induced ISI [5]. The architecture proposed in this paper uses knowledge of the instantaneous stochastic Green's function, so called *channel state information* (CSI), to reject interference caused by multipath. More specifically, the proposed architecture uses CSI to optimally predistort the transmitted waveform while using coherent detection with optimal spatial recombination to mitigate multipath interference, thereby minimizing bit error rate (BER). This architecture consists of one transmit and one receive plane array with sparse apertures, meaning apertures in each plane are placed at least one coherence length apart and that each aperture diameter is smaller than a coherence length. The link range of this architecture is primarily limited by the need for up-to-date CSI at the transmitter, which is delayed at least by the amount of time required to measure and feed back the information. As a result, the maximum transmission distance is a function of the duration of time the channel impulse response is approximately constant, or coherence time, and the speed of sound in sea water. Experiments have shown coherence times of about one second for mid-to-high frequencies [6]. Thus, this architecture is limited to a link range of less than 1km by the low speed of sound and coherence time. This architecture can be applied for any transmitter-receiver plane orientation, including vertical as in submarines or underwater vehicles communicating with receivers at the sea surface (Fig. 2).

Many emerging applications in the ocean that require high-speed, reliable wireless communication have the potential to benefit from the proposed architecture. An example of such an application is a real-time ocean observation system, which is used more and more frequently to adaptively and optimally sample physical features of the ocean. Today, the number of autonomous ocean sensing vehicles used in semi-coordinated

operations is often larger than three and this number is rapidly increasing [7], [8], [9], [10]. For intelligent sensing with these vehicles, reliable high rate communications are needed. Predictions with uncertainties and data assimilation [11], [12] can be utilized to plan the sensing expected to be most useful. Such planning of optimal vehicle paths is referred to here as *path planning*. When path planning is also a function of the data to be sampled, the term *adaptive sampling* (Fig. I) is used [13]. For intelligent coordination among vehicles, information must be exchanged on multiple levels. Two-way communications over varied distances and bit rates are required among vehicles, from vehicles to ships or other surface crafts, and/or from vehicles to shore and command and control.

The new acoustic communication systems discussed in this paper would enhance such communications and would enable more intelligent and coordinated autonomous operations. The schemes recently developed for autonomous ocean sensing via adaptive sampling, path planning and onboard routing would readily benefit. Such schemes include: coordinated adaptive sampling with non-linear predictions of error reductions [13], [14]; Mixed Integer Linear Programming (MILP) for path planning [15]; nonlinear path planning using genetic algorithms [16]; dynamic programming and onboard routing for path planning [17]; command and control of assets over the web, directly from model instructions [18]; and strategies for fastest transit and routing [19]. Applications abound in a variety of fields including ocean science and engineering; ocean energy; ecosystem-based management; coastal monitoring, undersea surveillance, homeland security and harbor protection; and multi-scale climate monitoring and prediction.

Other applications that could potentially benefit from the proposed architecture include submarines communicating with ships at the sea surface and underwater vehicles communicating with other vehicles within a fleet. Additionally, long distance communication can be accomplished via multihopping, as multiple hops over several short distances allow transmission at a higher rate than its single-hop counterpart
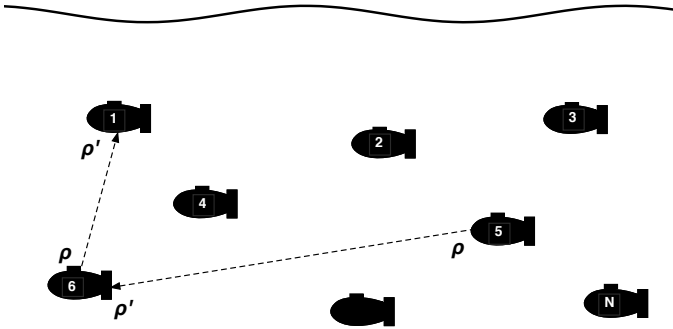
Fig. 4. In an undersea network, several underwater vehicles communicate to all or some of the other underwater vehicles. Thus, they act both as receive $\rho\prime$ and transmit ρ planes.
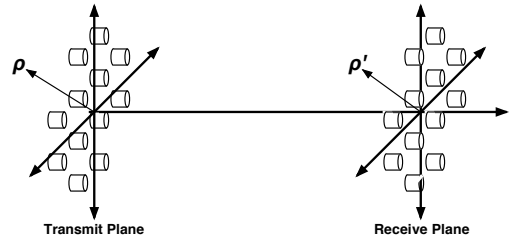

Fig. 5. Sparse aperture system geometry: Transmit and receive plane (consisting of apertures) at some depth below the sea surface. Orientation of the system under the water is not assumed to be horizontal.

[2]. Generally, this architecture can also be applied to an underwater network (Fig. 4) with transmission between each vehicle and a central source, or between each pair of vehicles, so that each vehicle acts both as a receiver and transmitter.

In Sec. II, we describe the system geometry and discuss the applicability of the architecture in the ocean environment. Additionally, we describe the optimal modulation, detection, and channel measurement scheme in terms of the singular value decomposition (SVD) of the instantaneous stochastic Green's function. In Sec. III, we derive asymptotic distribution of the system singular values and present a detailed discussion of the relevance of the theory to a wide range of real-world applications. Next, we show that the detected interference power decreases proportional to the inverse of the number of receivers. Using the theories describing asymptotic singular value distribution and interference power as a function of receivers, we derive an analytic closed-form expression for optimal system performance in terms of BER. We also prove the modulation and detection scheme provided in Sec. II achieves the optimal performance as the number of receive apertures approaches infinity. Further, we show very good agreement between a Monte Carlo simulation and theoretical results. This is followed by a conclusion in Sec. IV.

II. SYSTEM DESCRIPTION

The system geometry consists of a transmit plane ρ with n_{tx} apertures and a receive plane ρ' with n_{rx} apertures. For this paper, we use the term *transmit aperture* to mean transmit acoustic emitter and *receive aperture* to mean a receive hydrophone. We define a pair of ancillary variables, $n_{min} = \min(n_{tx}, n_{rx})$ and $n_{max} = \max(n_{tx}, n_{rx})$, which arise often in the following analysis. The transmit and receive plane are assumed to be parallel with an origin along a common axis. Location and orientation of the system in the open ocean is kept general without restriction on distance from sea surface or floor. We assume the apertures in each plane are placed at least one coherence length apart, ensuring the $n_{tx}n_{rx}$ links are uncorrelated. For a propagation distance of 800m and a signal between 15-35kHz, experimental data has suggested a coherence length of 35cm [1]. Thus requiring the

apertures to be a coherence length apart does not create a spatially prohibitive plane array. Additionally, we assume each aperture diameter is smaller than a coherence length. We refer to this geometry as a *sparse aperture system* (Fig. 5).

Coherence length depends on the conditions and physical processes of the ocean. Strong turbulence decreases the coherence length, as two points close in space are not strongly related.

We assume a coherent narrowband wave, with center wavelength λ, is transmitted from the ρ plane, propagates over z meters, and is detected at the receive plane ρ'. The field is detected coherently using either a heterodyne or homodyne receiver. Also, we assume the channel state is fully known by the transmitter. We will discuss methods of estimating the channel state at the end of this subsection.

We model the multipath interference as being a finite number of discrete rays. As such, the received field can be modeled as:

$$
\begin{aligned}
\mathbf{y}[n] &= \frac{\alpha^{(d)}}{\sqrt{n_{max}}}\mathbf{H}^{(d)}\mathbf{x}[n] + \mathbf{w}[n] + \\
&\quad \frac{\alpha^{(1)}}{\sqrt{n_{max}}}\mathbf{H}^{(1)}\mathbf{x}[n - \Delta_1] + ... + \frac{\alpha^{(m)}}{\sqrt{n_{max}}}\mathbf{H}^{(m)}\mathbf{x}[n - \Delta_m] \\
&= \mathbf{y}^{(d)}[n] + \mathbf{y}^{(1)}[n] + ... + \mathbf{y}^{(m)}[n] + \mathbf{w}[n]
\end{aligned}
$$
(1)

where $\mathbf{x}[n] \in \mathbb{C}^{n_{tx}}$ is a vector representing the transmitted field at time n, $\mathbf{y}[n] \in \mathbb{C}^{n_{rx}}$ is a vector representing the received field at time n, and $\mathbf{w}[n] \in \mathbb{C}^{n_{tx}}$ represents additive white circularly symmetric complex Gaussian noise received at time n. $\alpha^{(d)} \in \mathbb{R}$ is the path attenuation for the direct path and $\alpha^{(k)} \in \mathbb{R}$ is the path attenuation for the kth multipath component. The direct channel is represented by $\mathbf{H}^{(d)} \in \mathbb{C}^{n_{rx} \times n_{tx}}$: element $h_{ij}^{(d)}$ of $\mathbf{H}^{(d)}$ is the direct path gain from the ith transmit aperture to the jth receive aperture. The matrices $\mathbf{H}^{(k)}, k \in \{1, ..., m\}$ represent the multipath interference: element $h_{ij}^{(k)}$ is the gain of the kth reflected (or refracted) path from the ith transmit aperture to the jth receive aperture. Δ_i is the time of arrival of multipath component i measured from the time of arrival of the direct path. The path delay may be positive or negative because a multipath ray can

travel at a higher speed than the direct ray. The terms of the second equality in (1) are defined as:

$$\mathbf{y}^{(d)}[n] = \frac{\alpha^{(d)}}{\sqrt{n_{max}}}\mathbf{H}^{(d)}\mathbf{x}[n]$$

$$\mathbf{y}^{(1)}[n] = \frac{\alpha^{(1)}}{\sqrt{n_{max}}}\mathbf{H}^{(1)}\mathbf{x}[n - \Delta_1]$$

$$\vdots \quad \vdots \qquad \vdots \tag{2}$$

$$\mathbf{y}^{(m)}[n] = \frac{\alpha^{(m)}}{\sqrt{n_{max}}}\mathbf{H}^{(m)}\mathbf{x}[n - \Delta_m]$$

where $\mathbf{y}^{(d)}[n]$ is the received field due to the direct path and $\mathbf{y}^{(k)}[n]$ is the received field due to the kth multipath component.

We have implicitly invoked Taylor's frozen turbulence hypothesis [20] by assuming $\mathbf{H}^{(d)}$ is time invariant. This is true if the bit period is much less than the oceanic coherence time, which occurs for the transmission range specified. The normalization $(n_{max})^{-1/2}$ is chosen to ensure:

- additional apertures will not increase the system power gain and
- that reciprocity is satisfied.

We decouple the input-output relationship of $\mathbf{H}^{(d)}$ with a singular value decomposition:

$$\frac{1}{\sqrt{n_{max}}}\mathbf{H}^{(d)} = \mathbf{U}\boldsymbol{\Gamma}\mathbf{V}^{\dagger} \tag{3}$$

where the ith column of $\mathbf{U}$ is an output eigenmode, the ith row of $\mathbf{V}$ is an input eigenmode, and the i, ith entry of the diagonal matrix $\boldsymbol{\Gamma}$ is the singular value, or diffraction gain, associated with the ith input/output eigenmode. We use $(\cdot)^{\dagger}$ as the conjugate transpose. For the context of this paper, an *eigenmode* is a particular spatial field distribution, or spatial mode. We will denote the diffraction gain associated with the ith eigenmode as γ_i so that:

$$\tilde{y}_i = \gamma_i \tilde{x}_i + \tilde{w}_i \tag{4}$$

where $\tilde{\mathbf{x}}$, $\tilde{\mathbf{y}}$, and $\tilde{\mathbf{w}}$ are related to $\mathbf{x}$, $\mathbf{y}$, and $\mathbf{w}$ through the usual SVD, such as in [21]. Note $\tilde{w}_i$ retains its circularly symmetric complex Gaussian distribution. We have not included the multipath components in (4).

Binary phase shift keying (BPSK) is a common modulation scheme for acoustic communication systems with coherent detection. Though results developed here may easily be applied to other modulation schemes (e.g. binary on-off keying, frequency shift keying, quadrature modulation, etc.), we will limit ourselves to the discussion of BPSK systems for brevity. We will show that the optimal scheme to minimize BER using BPSK is to allocate all power to the input eigenmode associated with the maximum singular value. To transmit a bit $C[n] \in \{0, 1\}$ with power E_t, the optimal transmit field is simply:

$$\mathbf{x}[n] = \mathbf{v}_{max}\sqrt{E_t}e^{i\pi C[n]} \tag{5}$$

where $\mathbf{v}_{max}$ is the input eigenmode associated with the largest singular value. The associated optimal spatial recombination scheme is:

$$\phi[n] = \Re e\{\mathbf{u}_{max}^{\dagger}\mathbf{y}[n]\} \tag{6}$$

where $\phi[n]$ is a sufficient statistic at time n and $\mathbf{u}_{max}$ is the output eigenmode associated with the largest singular value. We will prove the optimality of this modulation and detection scheme in the next section.

The channel state can be measured by transmitting an impulse from each transmitter sequentially and recording the time variation of the received field at each receiver. From this measurement, we can build up a channel transfer matrix as a function of time. We can then assign the time instance with the largest power gain to $\mathbf{H}^{(d)}$. In practice, we do not need to calculate the multipath transfer matrices. They can be measured, if desired, by selecting the time instances with the $m + 1$ largest power gains, corresponding to the direct propagation path and m multipath components, and creating $\mathbf{H}^{(d)}$ and $\mathbf{H}^{(k)}$. The need to compute the SVD and feed back some information regarding the direct path transfer matrix $\mathbf{H}^{(d)}$ limits the distance from the transmit plane to the receive plane to be under 1000m. Time to compute the transfer matrix is small compared to the propagation time, an important consideration for implementation. Propagation attenuation over this distance limits available carrier frequencies to 10kHz to 30kHz.

We have presented an idealized channel measurement scheme. However, other methods are likely more feasible for implementation. For instance, a system could establish an initial channel state estimate via a full channel measurement and subsequently track channel state perturbations with time, thus taking advantage of current information to reduce the number of channel measurements. This method is effective provided the tracking bandwidth is much higher than oceanic temporal coherence bandwidth. Because the apertures are sparse (transmitters and receivers in each place are at least a coherence length apart), $n_{rx} \times n_{tx}$ channel measurements are needed to fully characterize the ocean state (i.e. populate $\mathbf{H}^{(d)}$).

III. PERFORMANCE OF SPARSE APERTURE SYSTEMS

In this section we present the performance of sparse aperture acoustic systems with wavefront control and coherent detection. Specifically, we present the asymptotic singular value distribution, multipath rejection performance, and asymptotic BER.

A. Singular Value Distribution

The transfer function $h_{ij}^{(d)}$ describing propagation through random media can be represented as the deterministic free-space Green's function h_{ij}^{FS} modified by amplitude χ_{ij} and phase ϕ_{ij} perturbation terms:

$$h_{ij}^{(d)} = h_{ij}^{FS}\chi_{ij}e^{i\phi_{ij}} \tag{7}$$

In the random field of the underwater acoustic channel, χ_{ij} and ϕ_{ij} are random variables. Assuming the entries of $\mathbf{H}^{(d)}$ are

independent and identically distributed (i.i.d.), we can find the probability density function (pdf) governing the distribution of the system singular values.

Theorem 3.1: Assuming the entries of $\mathbf{H}^{(d)}$ are i.i.d., the pdf of diffraction gains, γ_i^2, for a single ocean state, as the number of transmit apertures and receive apertures asymptotically approaches infinity, converges almost surely to the Marcenko-Pastur density:

$$f_\beta(x) =$$
$$(1-\beta)^+ \delta(x) + \frac{\sqrt{\left(x - (1-\sqrt{\beta})^2\right)^+ \left((1+\sqrt{\beta})^2 - x\right)^+}}{2\pi x}$$
$$(8)$$

where $\beta = \dfrac{\min(n_{rx}, n_{tx})}{\max(n_{rx}, n_{tx})}$ and $(x)^+ = \max(x, 0)$.

Proof. A nice proof of the Marcenko Pastur density for i.i.d. matrices can be found in [22]. $\square$

Fig. 6 shows the Marcenko Pastur density for various system geometries.

As stated in the theorem, the entries of $\mathbf{H}^{(d)}$ must be i.i.d. for the Marcenko Pastur density to describe the singular value distribution. We now include a discussion that reasons that the entries of $\mathbf{H}^{(d)}$ are in fact approximately i.i.d. for many realistic applications.

Because each ray traverses a different path from transmitter i to receiver j, the entries of $\mathbf{H}^{(d)}$ will be uncorrelated provided transmit/receive apertures are separated by at least a coherence length. It is difficult to prove independence, so we assume that uncorrelated implies independence.

The transmission range is much larger than typical acoustic wavelengths for this system (5-15cm), so the far field approximation is valid and the difference between amplitude variations among paths is negligible. Additionally, the transmission range is much larger than the distance between transmit and receive apertures. Fig. 7 shows the maximum array size possible for the limiting case when the longest and shortest direct propagation paths from transmitter to receiver differ by 10%. Even in the most limiting case of a 100m transmission range, the array extent is not restrictive. If all path lengths are within 10%, we estimate these path lengths as being the same, so that the amplitude statistics should also be the same for each path. Consequently, χ_{ij} has approximately identical statistics for all (i, j) pairs.

ϕ_{ij} is some unknown continuous distribution with zero mean and variance σ_ϕ^2. For channels with sufficient turbulence, σ_ϕ^2 is much greater than 2π. Because the phase is purely real, it can always be represented as a value from 0 to 2π. Because the variance is very large compared to this range, the distribution can be approximated as uniform from 0 to 2π for all (i, j) pairs. Thus, ϕ_{ij} can also be approximated as identically distributed.

Additionally, h_{ij}^{FS} can be absorbed into the phase term, as it is a complex number which can be represented as $e^{i\phi_{ij}^{FS}}$ so that the transfer function now becomes $h_{ij} = \chi_{ij} e^{i\phi'_{ij}}$ where
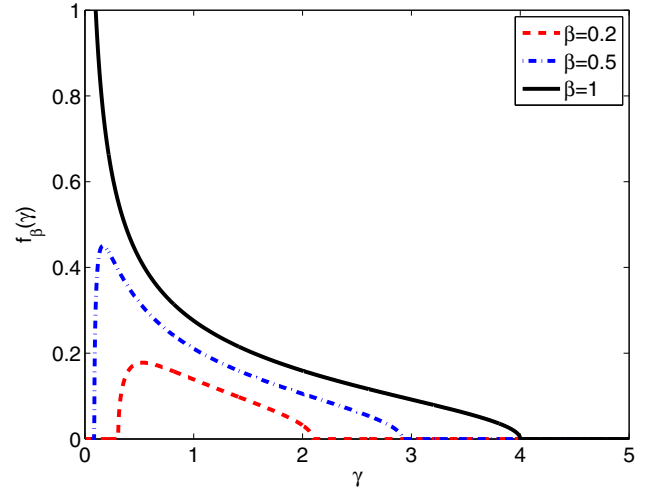

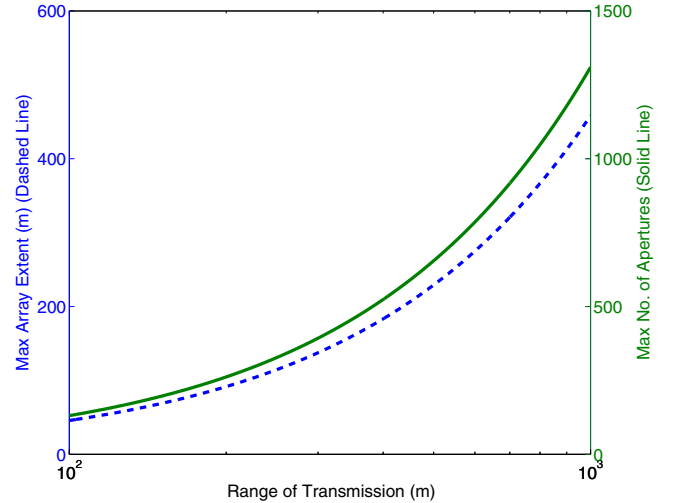Fig. 6. Marcenko Pastur asymptotic singular value probability density function.

Fig. 7. The maximum extent of the receive and transmit planes increases with propagation distance. This figure assumes a coherence length of 35cm.

$\phi'_{ij} = \phi_{ij} + \phi_{ij}^{FS}$. Without loss of generality, the expression is shown for $\lambda z = 1$. Again, because of the periodicity of the complex exponential $e^{i(\cdot)}$, this additive term does not change the distribution and it remains uniform from 0 to 2π. Thus, h_{ij} is modeled as a function of i.i.d. random variables.

Thm. 3.1 assumes a large number of apertures. Fig. 7 shows that this assumption is satisfied for physically realizable systems. For instance, if we have a link range of 100m, we can place up to 100 transmitters and 100 receivers and still meet all of the restrictions necessary for the theorem to apply. Therefore, the theory is applicable for any practical system.

As a corollary to Thm. 3.1, the number of eigenmodes corresponding to non-zero singular values converges, almost surely, to $\min(n_{tx}, n_{rx})$. Additionally, the maximum singular value converges, almost surely, to $\gamma_{max}^2 = (1 + \sqrt{\beta})^2$.

B. Multipath Rejection

Multipath interference severely limits acoustic communication systems. Previous work has focused on the use of equalizers [5] or vector receivers [1] to mitigate the multipath interference. The sparse aperture system effectively eliminates multipath induced ISI when there are many transmit and receive apertures. The system, however, does not collect power from multipath components, but only rejects it.

In this section, we show that multipath interference can be reduced to any desired level by increasing the number of transmitters and receivers. Further, we show that the detected interference power is proportional to $1/n_{rx}$. Formally, we wish to select a spatial modulation $\mathbf{x}[n]$ and receiver spatial recombination scheme S to minimize the BER or, equivalently, maximize the signal to interference noise ratio:

$$
\begin{aligned}
\mathbf{x}^*[n] &= \arg \min_{\mathbf{x}[n],S} Q\left(\sqrt{\frac{2E^{(d)}}{\sigma_w^2 + \sum_{k=1}^{m} E^{(k)}}}\right) \\
&= \arg \max_{\mathbf{x}[n],S} \left(\frac{E^{(d)}}{\sigma_w^2 + \sum_{k=1}^{m} E^{(k)}}\right)
\end{aligned} \tag{9}
$$

where σ_w^2 is the energy due to the noise $\mathbf{w}[n]$, $E^{(d)}$ is average detected signal energy and $E^{(k)}$ is the average detected energy in the kth multipath component. $Q(\cdot)$ is the q-function. We have assumed the waveform transmitted through a multipath channel contributes as noise through ISI. The optimization in (9) is very general. Specifically, $\mathbf{x}^*[n]$ would have nulls in the direction of multipath components if such a waveform was optimal. Further, the optimization will find the waveform that propagates most efficiently through the turbulent ocean. Thm. 3.2 gives the solution to (9) for the case with many transmit and receive apertures.

Theorem 3.2: As the number of transmit and receive apertures grows large, the spatial field distribution that minimizes BER, as formulated in (9), is given by:

$$
\mathbf{x}^*[n] = a[n]\mathbf{v}_{max} \tag{10}
$$

where we have used SVD, $\mathbf{H}^{(d)} = \mathbf{U}\boldsymbol{\Gamma}\mathbf{V}^\dagger$. Thus, $\mathbf{v}_{max}$ is the input eigenvector associated with the maximum singular value γ_{max} of $\mathbf{H}^{(d)}$. Data is encoded by time variation of $a[n] \in \mathbb{C}$, which is spatially constant at a particular time. For example, for BPSK $a[n] = \sqrt{E_t}e^{i\pi C[n]}$. A sufficient statistic for optimum detection is:

$$
\phi[n] = \Re\{\mathbf{u}_{max}^\dagger \mathbf{y}[n]\} \tag{11}
$$

where $\phi[n]$ is a sufficient statistic at time n. The associated optimal probability of error is:

$$
P_{error} = Q\left(\sqrt{\frac{2\alpha^{(d)}\gamma_{max}^2 E_t}{\sigma_w^2 + \frac{E_t}{n_{rx}}\sum_{k=1}^{m}\alpha^{(k)}}}\right) \tag{12}
$$

Proof. To prove this theorem, we show that this scheme maximizes $E^{(d)}$ while at the same time minimizing $E^{(k)} \forall k$ for a large number of transmit and receive apertures. First, we

show that (10) maximizes $E^{(d)}$:

$$
\begin{aligned}
E^{(d)} &= \mathbb{E}[(\Re\{\mathbf{u}_{max}^\dagger \mathbf{y}^{(d)}[n]\})^2] \\
&= \frac{\alpha^{(d)}}{n_{max}}\mathbb{E}[(\Re\{\mathbf{u}_{max}^\dagger \mathbf{H}^{(d)}\mathbf{v}_{max}a[n]\})^2] \\
&= \frac{\alpha^{(d)}}{n_{max}}(\Re\{\mathbf{u}_{max}^\dagger \mathbf{H}^{(d)}\mathbf{v}_{max}\})^2 E_t \\
&= \alpha^{(d)}\gamma_{max}^2 E_t
\end{aligned} \tag{13}
$$

Because the SVD provides a complete orthonormal basis for the transmit and receive fields, the largest possible $E^{(d)}$ is γ_{max}^2. Thus we have shown that this scheme maximizes $E^{(d)}$. We now show that (11) asymptotically ($n_{rx} \to \infty$) drives the interference power $E^{(k)}$ to zero:

$$
\begin{aligned}
E^{(k)} &= \mathbb{E}[(\Re\{\mathbf{u}_{max}^\dagger \mathbf{y}^{(k)}[n]\})^2] \\
&= \frac{\alpha^{(k)}}{n_{max}}\mathbb{E}[(\Re\{\mathbf{u}_{max}^\dagger \mathbf{H}^{(k)}\mathbf{v}_{max}\})^2] \\
&= \alpha^{(k)}\mathbb{E}[(\Re\{\mathbf{u}_{max}^\dagger \tilde{\mathbf{v}}\})^2]
\end{aligned}
$$

where we have defined $\tilde{\mathbf{v}} = n_{max}^{-1}\mathbf{H}^{(k)}\mathbf{v}_{max}$. So, we can write:

$$
\begin{aligned}
E^{(k)} &= \alpha^{(k)}\mathbb{E}\left[\left(\Re\left\{\sum_{i=1}^{n_{rx}} u_{max,i}^\dagger \tilde{v}_i\right\}\right)^2\right] \\
&= \alpha^{(k)}\mathbb{E}\left[\left(\sum_{i=1}^{n_{rx}}\Re\left\{u_{max,i}^\dagger \tilde{v}_i\right\}\right)^2\right] \\
&= \alpha^{(k)}\mathbb{E}\left[\xi^2\right]
\end{aligned}
$$

where $u_{max,i}$ is element i of $\mathbf{u}_{max}$ and $\tilde{v}_i$ is element i of $\tilde{\mathbf{v}}$. We have defined $\xi = \sum_{i=1}^{n_{tx}}\Re\left\{u_{max,i}^\dagger \tilde{v}_i\right\}$. The entries of $\mathbf{H}^{(k)}$ are identically distributed, independent of each other, and independent of the entries of the direct channel matrix $\mathbf{H}^{(d)}$. The entries of $\mathbf{H}^{(k)}$ are independent of the entries of $\mathbf{H}^{(d)}$ because the multipath components traverse a different path from the direct component and therefore experience different fading. The central limit theorem can be applied to the summation because the terms in the summation, $\Re\left\{u_{max,i}^\dagger \tilde{v}_i\right\}$, are independent. As the number of receive apertures grows large, the central limit theorem implies:

$$
\xi \sim N\left(0, \frac{1}{n_{rx}}\right)
$$

And as a result:

$$
E^{(k)} = \frac{\alpha^{(k)}}{n_{rx}} \tag{14}
$$

We prove (12) by substituting (14) and (13) into (9). $\square$

In essence the receiver (11) is tuned to detect only the direct mode. As we increase the number of receive apertures, the tuner becomes increasingly narrow. As a result multipath components become less and less likely to couple into the direct mode tuned receiver. Nice intuition arises from an abstract vector space interpretation. The n_{rx}-dimensional vector space is the closed set of all possible receive fields. We can view the received field vector as the summation of the direct field

vector, the multipath field vectors, and the noise vector. The sufficient statistic in (11) is interpreted as an inner product between the received field vector and the direct field vector. The multipath field vectors have random orientation with respect to the direct field vector. As a result, the expected inner product between the multipath field vectors and the direct field vector becomes small as the vector space dimension increases. Thus, the multipath interference is rejected.

C. Asymptotic Bit Error Rate

For the optimal modulation scheme presented in Sec. II, the turbulence average BER is:

$$\Pr(error)$$
$$= \int_0^\infty Q \left(\sqrt{\frac{2\alpha^{(d)}\gamma_{max}^2 E_t}{\sigma_w^2 + \frac{E_t}{n_{rx}} \sum_{k=1}^m \alpha^{(k)}}} \right) f'_\beta(\gamma_{max}^2) d\gamma_{max}^2 \tag{15}$$

where $f'_\beta(\gamma_{max}^2)$ is the pdf of the largest singular value. This result is general for any sparse aperture communication system, but depends on the pdf of the largest singular value, $f'_\beta(\gamma_{max}^2)$, which is in general unknown. However, the pdf is known in the asymptotic case. As the number of apertures grows large, the pdf of the largest singular value converges, almost surely, to:

$$\lim_{n_{rx} \to \infty} f'_\beta(\gamma_{max}^2) = \delta \left(\gamma_{max}^2 - \left(1 + \sqrt{\beta}\right)^2 \right) \tag{16}$$

where $\delta(\cdot)$ is the Dirac delta. Using (16) to evaluate (15) provides a closed-form expression for the probability of error:

$$\lim_{n_{rx} \to \infty} \Pr(error)$$
$$= \int_0^\infty Q \left(\sqrt{2\gamma_{max}^2 \frac{\alpha^{(d)} E_t}{\sigma_w^2}} \right) \delta \left(\gamma_{max}^2 - \left(1 + \sqrt{\beta}\right)^2 \right) d\gamma_{max}^2$$
$$= Q \left(\sqrt{2 \left(1 + \sqrt{\beta}\right)^2 \frac{\alpha^{(d)} E_t}{\sigma_w^2}} \right) \tag{17}$$

For the asymptotic case, the interference power is completely rejected by the receiver. As such, the interference terms $E^{(k)}$ do not enter into the equation.

While this result is only exact in the asymptotic case, it provides a very good approximation for finite but large number of apertures. The $\left(1 + \sqrt{\beta}\right)^2$ term is the power gain over a system without the wavefront predistortion. This power gain term results from the ability to allocate all of the system transmit power into the spatial mode with the best propagation performance. Essentially, we select the mode with the best constructive interference for the particular receive aperture geometry and ocean state.

D. Discussion

Using the monotonicity of the Q-function, it is easy to prove that the optimum system is balanced, using the same number of transmit apertures and receive apertures. For a balanced system, setting $\beta = 1$ yields a power gain of four. This result is intuitively satisfying. Consider two scenarios: first, if there are more transmit apertures than receive apertures, the system can form more spatial modes than it can resolve and degrees of freedom are unused. Similarly, if there are more receive apertures than transmit apertures, the system can resolve more spatial modes than it can form and, again, degrees of freedom are unused. As a result, our intuition suggests a balanced system is optimal.

As the number of receive apertures becomes much larger than the number of transmit apertures, or vice-versa, $\beta \to 0$ and the system performance approaches that of the system without wavefront predistortion. This is also an expected result: as the system becomes very asymmetric, the ability to predistort the wavefront is lost.

The gain, in terms of probability of error, of moving to a diversity system with wavefront predistortion is:

$$\frac{\Pr(error|sparse\ aperture)}{\Pr(error|no\ diversity)} = e^{-3SNR} \tag{18}$$

At high SNR, using the sparse aperture system provides a large gain in BER compared to the no diversity system. At low SNR, the advantage of the more sophisticated system is less pronounced.

It is clear, in the asymptotic case, that the turbulence average BER does not depend on turbulence strength. Effectively, the many, many apertures act to average out the spatial variation induced by ocean turbulence. Turbulence strength does factor into the system design; in stronger turbulence, apertures may be placed closer together while in weaker turbulence, they must be placed farther apart. Further, stronger turbulence causes slower convergence to the Marcenko Pastur density; which means more apertures are required for (17) to be valid.

Lastly, as the total aperture size increases for a single aperture system, the power gain saturates as the aperture size approaches the coherence length. We have shown that the sparse aperture system, however, does not saturate with total aperture size. Indeed, the number of apertures used is only limited by form factor constraints, not ocean constraints.

E. Simulation

A Monte-Carlo simulation was performed to validate the theoretical results presented in (17). In the simulation, we assumed that the instantaneous ocean state was available at the transmitter. For a single ocean state, an equiprobable binary source was encoded according to (5), transmitted through the simulated ocean channel, detected coherently, and the number of raw bit errors recorded. The channel was assumed to have one multipath component with no attenuation relative to the direct path ($\alpha^{(k)} = 1$). This process was repeated many times with independent realizations of the ocean to arrive at the turbulence average BER presented in Fig. 8. In the figure, we show theory and simulation versus SNR, or $\alpha^{(d)} E_t / \sigma_w^2$. The number of transmitters was 100, 100, 200 and the number of receivers was 100, 50, 100 giving $\beta = 1$, $\beta = 0.5$, and $\beta = 0.1$.
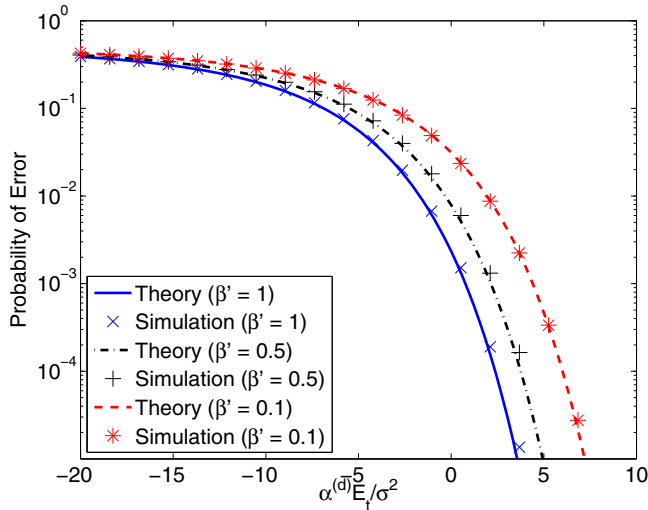
Fig. 8. BER vs SNR - A comparison of Monte-Carlo simulation and theory for binary phase shift keying.

From the figure, we see very good agreement between theory and simulation. As we stated earlier, the theory provides an approximate solution to any system with a large but finite number of apertures. Here, we see the approximation is very close to the theory.

IV. CONCLUSION

High-frequency acoustic transmission over the ocean channel has the potential to provide intermediate range communication links for a myriad of applications. Such communication, however, is prone to long (up to 1s) and deep (10-20dB) fades and is susceptible to multipath induced ISI. In this paper, we have shown that a sparse aperture transmitter and receiver system with wavefront predistortion provides protection against fading and multipath interference in addition to better performance (average BER) compared with a single aperture system.

We showed that using receiver channel state information is feasible for intermediate range acoustic communication links (up to 1km). Further we showed, for this link, that the number of sparse apertures can practically be made large enough so that asymptotic results approximate finite results well. We presented spatial modulation at the transmitter and spatial recombination at the receiver that asymptotically minimize BER. This optimal scheme in fact transmits the spatially modulated waveform that propagates with the smallest diffraction loss while, at the same time, reduces multipath interference to any level desired. Additionally, we showed that the interference noise power is reduced proportional to $1/n_{rx}$. Finally, we calculated the asymptotic BER for the sparse aperture acoustic system.

For many current and emerging applications, the data rate provided by acoustic communication is less than desired. As such, future work might explore increasing the data rate by modulating multiple spatial modes simultaneously. Coding across the multiple spatial modes can provide a capacity achieving architecture. The derivation of the channel capacity will likely follow the wireless communication derivation for MIMO capacity found by [23]. We expect the additional complexity required to implement a system that communicates over multiple spatial modes to be justified by requirements of emerging systems.

Other work could include an analysis of the effect of vehicle velocity on link range. As vehicle velocities increase, the link range will decrease because the observed channel state changes more quickly than the coherence time. Additionally, in most applications, system requirements on BER will determine the number of transmitters and receivers. However, in the absence of this constraint, establishing an optimal number of transmitters/receivers in terms of BER per unit cost remains an open research question.

REFERENCES

[1] D. B. Kilfoyle, and A. B. Baggeroer, "The State of the Art in Underwater Acoustic Telemetry," *IEEE Journal of Oceanic Engineering*, vol. 25, pp. 4-29, January 2000.

[2] M. Stojanovic, "Underwater Wireless Communications: Current Achievements and Research Challenges," in *IEEE Oceanic Engineering Society Newsletter*, vol. XXXXI, no. 2, Spring 2006.

[3] S. Arnon and D. Kedar, "Non-line-of-sight underwater optical wireless communication network," *Journal of the Optical Society of America A*, vol. 26, pp. 530-539, March 2009.

[4] N. M. Carbone, "Effects of Tidally Driven Temperature Flucuations on Shallow-Water Acoustic Communications at 18kHz," *IEEE Journal of Oceanic Engineering*, vol. 25, pp. 84-94, January 2000.

[5] M. Stojanovic. "Underwater Acoustic Communication," *Wiley Encyclopedia of Electrical and Electronics Engineering*. J. G. Webster, Ed., John Wiley & Sons, 1999, vol. 22, pp. 688-698.

[6] M. Baidey, "Signal Variability in Shallow-Water Sound Channel." *IEEE Journal of Oceanic Engineering* vol. 25, pp. 492-500, October 2000.

[7] T. B. Curtin, J. G. Bellingham, "Progress toward autonomous ocean sampling networks," *Deep Sea Research Part II: Topical Studies in Oceanography*, In Press.

[8] N. E. Leonard, D. Paley, F. Lekien, R. Sepulchre, D. M. Fratantoni, and R. Davis, "Collective motion, sensor networks and ocean sampling," *Proceedings of the IEEE*, vol. 95, pp. 1-27, 2007.

[9] P. J. Haley, Jr., P. F. J. Lermusiaux, A. R. Robinson, W. G. Leslie, O. Logutov, "Forecasting and Reanalysis in the Monterey Bay/California Current Region for the Autonomous Ocean Sampling Network-II Experiment," *Deep Sea Research Part II: Topical Studies in Oceanography*, special issue on AOSN-II, In Press, Corrected Proof, 2009.

[10] S. R. Ramp, R. E. Davis, N. E. Leonard, I. Shulman, Y. Chao, A. R. Robinson, J. Marsden, P. Lermusiaux, D. Fratantoni, J. D. Paduan, F. Chavez, F. L. Bahr, S. Liang, W. Leslie, and Z. Li, "Preparing to Predict: The Second Autonomous Ocean Sampling Network (AOSN-II) Experiment in the Monterey Bay," in *Deep Sea Research Part II: Topical Studies in Oceanography*, special issue on AOSN-II, In Press, Corrected Proof, 2009.

[11] P. F. J. Lermusiaux, C.-S. Chiu, G. G. Gawarkiewicz, P. Abbot, A. R. Robinson, R. N. Miller, P. J. Haley, W. G. Leslie, S. J. Majumdar, A. Pang and F. Lekien, "Quantifying Uncertainties in Ocean Predictions" in *Oceanography*, special issue on "Advances in Computational Oceanography", T. Paluszkiewicz and S. Harper, Eds., vol. 19, pp. 92-105, 2006.

[12] P. F. J. Lermusiaux, P. Malanotte-Rizzoli, D. Stammer, J. Carton, J. Cummings and A. M. Moore, "Progress and Prospects of U.S. Data Assimilation in Ocean Research" in *Oceanography*, special issue on "Advances in Computational Oceanography," T. Paluszkiewicz and S. Harper, Eds., vol. 19, pp. 172-183, 2006.

[13] P. F. J. Lermusiaux, "Adaptive Modeling, Adaptive Data Assimilation and Adaptive Sampling," in *Physica D*, special issue on "Mathematical Issues and Challenges in Data Assimilation for Geophysical Systems: Interdisciplinary Perspectives," C. K. R. T. Jones and K. Ide, Eds., vol. 230, pp. 172-196, 2007.

[14] P. F. J. Lermusiaux, P. J. Haley Jr. and N. K. Yilmaz, "Environmental Prediction, Path Planning and Adaptive Sampling: Sensing and Modeling for Efficient Ocean Monitoring, Management and Pollution Control," *Sea Technology*, vol. 48, pp. 3538. 2007.

[15] N.Yilmaz, C. Evangelinos, P. F. J. Lermusiaux, and N. M. Patrikalakis, "Path Planning of Autonomous Underwater Vehicles for Adaptive Sampling Using Mixed Integer Linear Programming,'" *IEEE Journal of Oceanic Engineering*, vol. 33, pp. 522-537, October 2008.

[16] K.D. Heaney, G. Gawarkiewicz, T.F. Duda, and P.F.J. Lermusiaux, "Non-linear optimization of autonomous undersea vehicle sampling strategies for oceanographic data-assimilation," *Journal of Field Robotics*, vol. 24, pp.437-448, 2007.

[17] D. Wang, P. F. J. Lermusiaux, P. J. Haley, D. Eickstedt, W. G. Leslie and H. Schmidt, "Acoustically Focused Adaptive Sampling and On-board Routing for Marine Rapid Environmental Assessment," in *Journal of Marine Systems*, special issue of the on "Coastal Processes: Challenges for Monitoring and Prediction," Drs. J.W. Book, Prof. M. Orlic and Michel Rixen (Guest Eds), In Press, 2009.

[18] J. Xu, P. F. J. Lermusiaux , P. J. Haley Jr. , W. G. Leslie and O. G. Logutov, "Spatial and Temporal Variations in Acoustic propagation during the PLUSNet07 Exercise in Dabob Bay," *Proceedings of Meetings on Acoustics*, vol. 4, 155th Meeting Acoustical Society of America, 2008.

[19] R. E. Davis, N. Leonard, and D. M. Fratantoni, "Routing strategies for underwater gliders." *Deep-Sea Research II*, 2008.

[20] G. I. Taylor, "The spectrum of turbulence," *Proc. R. Soc. Lond.*, Ser A 164, pp. 476490, 1938.

[21] D. Tse and P. Viswanath, *Fundamentals of Wireless Communication*. New York, NY: Cambridge University Press, 2005.

[22] Z. D. Bai, "Methodologies in spectral analysis of large dimensional random matrices, a review," *Statistica Sinica*, vol. 9, pp. 611-662, 1999.

[23] A. M. Tulino, A. Iozano and S. Verdú, "MIMO Capacity with Channel State Information at the Transmitter," in *IEEE International Symposium on Spread Spectrum Techniques and Applications*, 2004, pp. 23-26.